JOC*Note*

Redox Regulation of Helical Structures in Short Peptides with an Intramolecular Ferrocenyl Cross-Linking Agent

Kazuhisa Fujimoto,* Hirokazu Kawai, Miwo Amano, and Masahiko Inouye*

Graduate School of Pharmaceutical Sciences, University of Toyama, Sugitani 2630, Toyama 930-0194, Japan

fujimoto@pha.u-toyama.ac.jp; inouye@pha.u-toyama.ac.jp

Received January 25, 2008

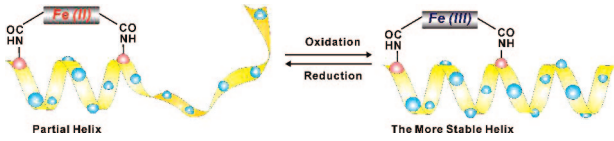

We redox-regulated α-helicity of short peptides intramolecularly cross-linked with a ferrocenyl linker between amino acid side chains. The helical content of the cross-linked peptide was estimated to be 56% in the neutral state of the ferrocene core at 25 °C. The addition of an oxidant to the solution of the cross-linked peptide enhanced the helicity up to 75%. The increased helical content returned to the same level as that in the previous ferrocene state by further addition of a reductant.

Stable α-helices in short peptides are expected to behave as biologically active molecular pieces,[1] which can be used in applications such as peptide drugs and peptide inhibitors. Therefore, a variety of peptides with stable helical structures have been developed by salt bridging between acidic and basic amino acid residues, introducing non-natural amino acids, cross-linking between the side chains of amino acid residues, etc.[2] Besides helical stabilization, the reversible regulation of helical structures in short peptides by external physical stimuli is an attractive subject of research. Such structural regulation will realize the operation of biological recognition events by the stimuli at will, in which α-helices participate.[3]

We have recently reported the reversible photoregulation of α-helices in short peptides by using a photochromic cross-linking agent containing a spiropyran core.[4] The short peptides are intramolecularly cross-linked with the agent between two Lys residues. In addition to the photoregulation of the resulting helix, a "*trigger effect*" has been observed; by this effect, a partial helix formed by the cross-linking reaction at the N-terminus of the short peptides can induce the entire helicity. The structural change of the terminal spiropyran moiety might communicate with the dipole moment in the helices so that the entire helicity is photoregulated. In α-helices, the dipole moment is known to be directed from the N- to the C-terminus along the helical axes.[5] Therefore, switching molecules studied in this work are suitable cross-linkers for regulating α-helical structures in short peptides. They are required to quickly respond to external physical stimuli and strongly influence the dipole moment. Taking this aspect into account, redox-active molecules were newly considered as cross-linkers. Since the electric characteristics of redox-active molecules dramatically change according to their reduced and oxidized states, their introduction into short peptides will ensure that such a change directly influences the dipole moment of the α-helices. Furthermore, when the cross-linked peptides bearing redox-active segments are immobilized on electrodes, their helical structures can be regulated by charge injection from the electrodes. Electroregulation is more easily applicable to on-chip technology than photoregulation, thereby extending the potential of our methodology over peptide arrays and peptide chips.

Ferrocene and its derivatives have successfully been utilized for constructing various supramolecules[6] and biosensing molecules.[7,8] In the redox behavior of ferrocene, its reduced (neutral) and oxidized (cationic) entities formally contain Fe(II) and Fe(III) states, respectively. A 1,1′-disubstituted ferrocene skeleton is envisaged to be a potent candidate as a cross-linker because the skeleton possesses structural symmetry and two substituents suitable for preparing the corresponding cross-linking agent. The schematic illustration in Figure 1 potentially indicates that a partial helix is formed at the N-terminus by the cross-linking reaction and that the helical content of the cross-linked peptide can be regulated by the communication of the redox-active ferrocene core with the dipole moment of the helix. Thus, we now report the redox regulation of helical structures in short peptides cross-linked with the ferrocenyl cross-linking agent.

The cross-linking agent **1** was prepared from commercially available 1,1′-ferrocenedicarboxylic acid and *N*,*N*′-disuccinimidyl carbonate. The sequences of peptides **A**−**C** shown in Figure 1 are the same as those used in our previous study for the photoregulation of α-helices. The peptides possess a common sequence from positions i to $i + 7$ at the N-terminus, where each set of two Lys residues denoted in red is placed at position $i/i + 7$ for the cross-linking reaction with **1**. A comparison of

(1) Sewald, N., Jakubke, H.-D. , Eds. *Peptides: Chemistry and Biology*; Wiley-VCH: Weinheim, 2002.
(2) Recent reviews: (a) Errington, N.; Iqbalsyah, T.; Doig, A. J. In *Protein Design: Methods and Applications (Methods in Molecular Biology)*; Guerois, R., Lopez De La Paz, M., Eds.; Humana Press Inc.: Totowa, 2006; pp 3−26. (b) Doig, A. J.; Errington, N.; Iqbalsyah, T. In *Protein Folding Handbook Volume 1*; Buchner, J., Kiefhaber, T., Eds.; Wiley-VCH: Weinheim, 2005; pp 247−313. (c) Licini, G.; Prins, L. J.; Scrimin, P. *Eur. J. Org. Chem.* **2005**, 969–977.
(3) Woolley, G. A. *Acc. Chem. Res.* **2005**, *38*, 486–493.
(4) Fujimoto, K.; Amano, M.; Horibe, Y.; Inouye, M. *Org. Lett.* **2006**, *8*, 285–287.
(5) (a) Lockhart, D. J.; Kim, P. S. *Science* **1993**, *260*, 198–202. (b) Shoemaker, K. R.; Kim, P. S.; York, E. J.; Stewart, J. M.; Baldwin, R. L. *Nature* **1987**, *326*, 563–567.
(6) (a) Raymo, F. M. *Angew. Chem., Int. Ed.* **2006**, *45*, 5249–5251. (b) Osakada, K.; Sakano, T.; Horie, M.; Suzaki, Y. *Coord. Chem. Rev.* **2006**, *250*, 1012–1022.
(7) Willner, I., Katz, E., Eds. *Bioelectronics*; Wiley-VCH: Weinheim, 2005.
(8) Recent examples for detecting enzyme reactions and DNAs:(a) Li, D.; Gill, R.; Freeman, R.; Willner, I. *Chem. Commun.* **2006**, 5027–5029. (b) Sato, S.; Hokazono, K.; Irie, T.; Ueki, T.; Waki, M.; Nojima, T.; Kondo, H.; Takenaka, S. *Anal. Chim. Acta* **2006**, *578*, 82–87. (c) Inouye, M.; Ikeda, R.; Takase, M.; Tsuri, T.; Chiba, J. *Proc. Natl. Acad. Sci. U.S.A.* **2005**, *102*, 11606–11610.

10.1021/jo800117q CCC: $40.75
Published on Web 06/11/2008

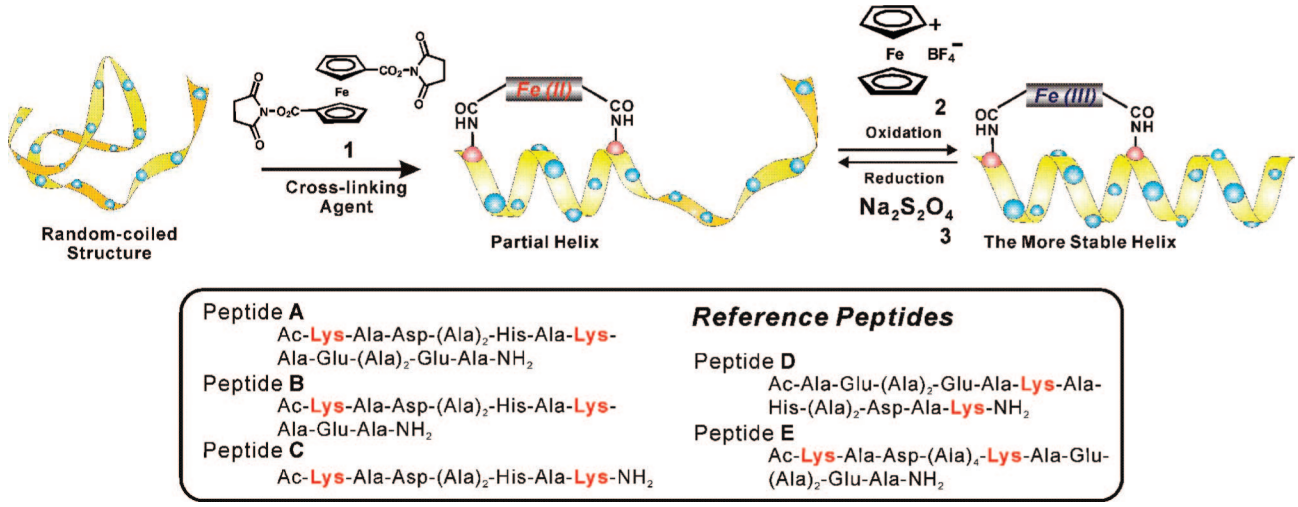

FIGURE 1. Stabilization of helical structures in short peptides with a ferrocenyl cross-linking agent **1** and switching of the helical contents by oxidation/reduction processes. Peptide sequences used in this study (inset).

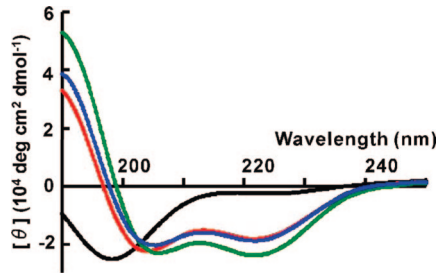

FIGURE 2. CD spectra of the native peptide **A** (5.0×10^{-4} M, black) and the cross-linked peptide **A·1** (5.0×10^{-4} M) in a 100 mM phosphate buffer (pH 7.0) at 25 °C using a cuvette cell with a 1 mm path length: Fe(II) state (red) of **A·1**, Fe(III) state after addition of **2** (green), and Fe(II) state (blue) after further addition of **3**.

the length of the $i/i + 7$ pitch on the α-helices with the distance between the two Cp rings of ferrocene reveals that the former (ca. 1.1 nm between two Lys C^{α}-atoms) is longer than the latter (ca. 0.3−0.7 nm). However, the alkyl side chains of the two Lys residues are considered for estimating the overall length of the resulting cross-linker, which implies that the length of the cross-linking agent should be shorter than that of the targeted pitch.[9] Additionally, the internal rotation of the Cp rings with respect to each other might aid the ferrocene core to adopt a favorable conformation for stabilizing the helices.[10] The cross-linking reaction of short peptides with **1** and the identification of the cross-linked peptides were carried out according to the previously reported procedures.[4]

To examine the redox regulation of the cross-linked peptides, the CD spectra of the native **A** and cross-linked **A·1** were measured in a 100 mM phosphate buffer (pH 7.0) at 25 °C (Figure 2). These spectra were measured at the concentration of 5.0×10^{-4} M because the ellipticities of the **A·1** obey Beer's law at $\leq 1.0 \times 10^{-3}$ M (Figure S1 in the Supporting Information). All of the helical contents were calculated on the basis of the mean residue ellipticity at 222 nm.[11] The native **A** takes an almost random-coiled structure (≤10% helicity), while the helical content of **A·1** increased up to 56% in the neutral Fe(II) state of ferrocene. The cyclic voltammetry (CV) of **A·1** was measured to select an appropriate oxidant in this study by scanning from −0.20 to +0.80 V vs Ag/AgCl in 100 mM $NaBF_4$ as an electrolyte. Initially, no CV peak was confirmed in the case of the native **A**. When applying **A·1** to CV, we observed an anodic peak potential $E_{pa} = +0.20$ V, which is lower than that for ferrocene (Figure S2 in the Supporting Information). The ferrocene core in **A·1** possesses two electron-withdrawing carboxamide groups; therefore, the lower E_{pa} value is of great interest to us and is still unexplained.[12] Among several oxidants soluble in water, ferrocenium tetrafluoroborate (**2**) is found to have a suitable E_{pa} value of +0.31 V. The addition of the oxidant **2** (1 equiv) to the aqueous solution of **A·1** caused a further increase in the helical content up to 75%. A switching efficiency of nearly 20% in the helical content is slightly higher than that observed in the previously reported photoregulation system (ca. 15%). The enhanced helicity might be due to a positive communication between the resulting cationic Fe(III) state in the ferrocenium core and the dipole moment of the helix. On the other hand, the CD spectrum of the native **A** remained unchanged upon addition of **2**. Unfortunately, no direct evidence was obtained for the oxidation of ferrocene to ferrocenium in **A·1** because of the overlap between the UV/vis spectra of the chromophores in **A·1** and **2**. To demonstrate the reversibility of the helical change in **A·1**, sodium dithionite (**3**) was used for reducing the ferrocenium core on **A·1**.[13] After the addition of **3** (1 equiv), the helical content of **A·1** returned to the same level as that in the previous ferrocene state. This switching behavior was reproducible under the same conditions as those mentioned above (not shown). However, a certain loss of the responsive ability was observed during the processes, probably because the consecutive addition of the redox agents contaminated the solution. No CD change was observed by the addition of **2** to the solution of **A·1** containing **3** beforehand.

To explore the effect of the cross-linkage at the N-terminus upon the redox regulation, a reference peptide **D** having the

(9) Fujimoto, K.; Kajino, M.; Inouye, M. *Chem.—Eur. J.* **2008**, *14*, 857–863.

(10) Inouye, M.; Hyodo, Y.; Nakazumi, H. *J. Org. Chem.* **1999**, *64*, 2704–2710.

(11) For the conversion of the ellipticity to the % helix, see:(a) Greenfield, N.; Fashman, G. D. *Biochemistry* **1969**, *8*, 4108–4116.

(12) A ferrocene dicarboxamide derivative, **Fc-(CO-Gly-OH)$_2$**, was prepared from 1,1′-ferrocenedicarboxylic acid and Gly, and its E_{pa} was found to be 0.60 V vs Ag/AgCl. As expected, ferrocenium tetrafluoroborate **2** was not able to oxidize **Fc-(CO-Gly-OH)$_2$** in CH_3CN. Thus, the low E_{pa} value of **A·1** might be due to the tight conformation of the ferrocene core in the cross-linked peptide.

(13) Wang, K.; Munoz, S.; Zhang, L.; Castro, R.; Kaifer, A. E.; Gokel, G. W. *J. Am. Chem. Soc.* **1996**, *118*, 6707–6715.

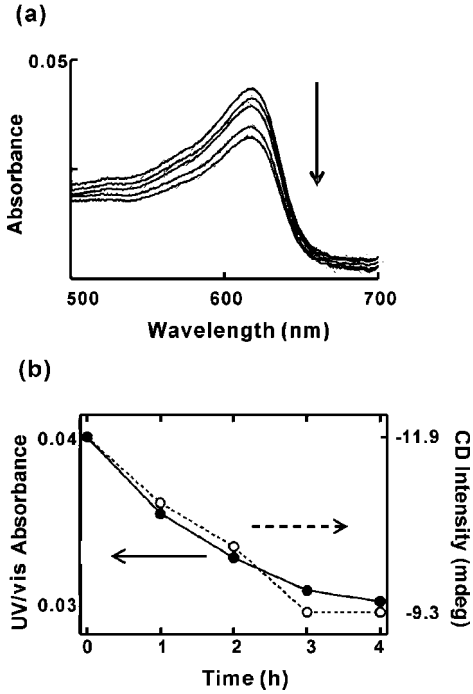

FIGURE 3. (a) UV/vis spectral changes of the cross-linked peptide **A·1** (5.0×10^{-4} M) in a 100 mM phosphate buffer (pH 7.0) after addition of **2** at 25 °C over a 4 h period and (b) spectral changes of the CD intensity at 222 nm (dashed line) and the UV/vis absorbance at 625 nm (solid line).

opposite sequence to that of peptide **A** was cross-linked with **1** at the C-terminus. The helical contents were estimated to be 16, 24, 32% for native **D**, cross-linked **D·1** in the neutral Fe(II) state, and cross-linked **D·1** in the cationic Fe(III) one, respectively (Figure S3 in the Supporting Information). In the reference peptide **D**, both of the helical stabilization and switching efficiencies are much lower as compared with those of peptide **A**. This finding indicates that the cross-linkage at the N-terminus is effective for the helical regulation.

Surprisingly, the increased CD intensity of **A·1**, caused by the formation of the ferrocenium core, decreased very gradually without the addition of **3** and became equal to that of the previous ferrocene state after ca. 4 h. To reveal this curious behavior, the UV/vis spectra of **A·1** were measured under the same conditions as those for the CD spectra. After the addition of **2** to the solution of **A·1**, the UV/vis absorbance at 625 nm from ferrocenium cations decreased gradually, as shown in Figure 3a, while no spectral change occurred in a buffer solution containing only **2**. The spectral changes of **A·1** for the UV/vis absorbance at 625 nm and the spectral changes of the CD intensity at 222 nm were both plotted as a function of time (Figure 3b). The time transition curves obtained from the CD and UV/vis measurements coincide well with each other. Thus, the time dependence of the CD transition is directly dominated by the reduction in the original ferrocenium state in **A·1**. We speculated that an amino acid residue existing in the cross-linked peptides caused this phenomenon. Therefore, peptide **E** was prepared, in which the His residue in peptide **A** was replaced by the Ala residue because the imidazole side chain in His is known to strongly coordinate with Fe(III) species, thereby perturbing their electronic circumstance.[14,15] After the addition

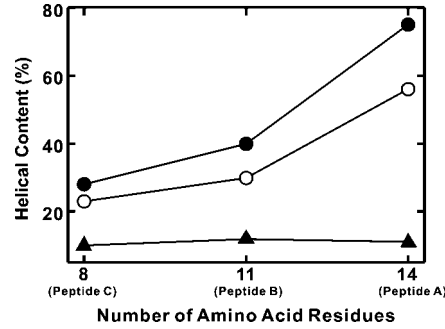

FIGURE 4. Relationship of the helical contents of native and cross-linked peptides with the peptide length: native peptide (closed triangle), peptide cross-linked with **1** in the Fe(II) state (open circle), and peptide cross-linked with **1** in the Fe(III) state (closed circle).

of the oxidant **2** to the solution of the cross-linked peptide **E·1**, the UV/vis absorbance at 625 nm barely changed over 4 h (not shown). Furthermore, when imidazole itself was added to the solution of **2** in CH_3CN, we observed a decrease in the absorbance at 625 nm (Figure S4 in the Supporting Information) and a visible color change in the solution of **2** from green to yellow. These findings imply that the His residue in **A·1** must be related to the gradual decrease in the CD intensity in the oxidized state of **A·1**, possibly due to the coordination of the imidazole side chain with the ferrocenium core or the intramolecular redox process between them.

The trigger effect described above was evaluated by comparing the helical contents of the cross-linked peptides **A**−**C**. The helical contents were plotted against the peptide length (Figure 4). In the cases of the native **A**−**C**, their helical contents are low and almost independent of their lengths. On the other hand, the helical contents of the cross-linked peptides increased significantly with an increase in the number of amino acid residues. The trigger effect is operative in both the present case and the case of using the photochromic cross-linking agent. Thus, the effect should be general to some extent for any short peptides and can be expected to lead to fruitful applications in biological investigations.

In conclusion, we have succeeded in the redox regulation of the helical structures in short peptides with the ferrocenyl cross-linking agent. The partial helix formed at the N-terminus in the peptides was found to induce the trigger effect as observed in the photoregulation system.[4] In the future, the switching of α-helices will be employed in on-chip chemistry, which is expected to open up the possibility of electroregulation of α-helices.

Experimental Section

General Methods and Materials. High-resolution mass spectra were obtained by the ESI-TOF method. ^{1}H and ^{13}C NMR spectra were recorded at 300 and 75 MHz, respectively.

Cross-Linking Agent 1. To a CH_3CN (1 mL) suspension of 1,1′-ferrocenedicarboxylic acid (100 mg, 0.38 mmol) and *N*,*N*′-disuccinimidyl carbonate (200 mg, 0.78 mmol) was added pyridine (60 μL) dropwise at room temperature. After being stirred at that temperature for 1 d, the mixture was poured into water. The resulting brown precipitate was filtered, washed with water and hexane, and dried to give **1**: yield 98% (175 mg); mp >270 °C (dec); IR (KBr) 1763, 1730 cm^{-1}; ^{1}H NMR (DMSO-d_6) δ 3.32 (s, 8 H), 4.92−4.93 (m, 4 H), 5.15−5.16 (m, 4 H); ^{13}C NMR (DMSO-

(14) Reddy, I. M.; Mahoney, A. W. *J. Agric. Food Chem.* **1995**, *43*, 1436–1443.

(15) Smith, D. M. A.; Dupuis, M.; Vorpagel, E. R.; Straatsma, T. P. *J. Am. Chem. Soc.* **2003**, *125*, 2711–2717.

d_6) δ 25.5, 66.2, 72.5, 75.7, 165.6, 170.2; HRMS (ESI) *m*/*z* calcd for $C_{20}H_{16}FeN_2NaO_8$ ([M + Na]$^+$) 491.0154, found 491.0140.

Solid-Phase Peptide Synthesis (SPPS). All peptides were synthesized by an automated peptide synthesizer using standard Fmoc chemistry. Peptides were constructed on an Fmoc-NH-SAL resin (capacity 0.59 mmol/g). After the SPPS, N-terminal amino groups were acetylated with 5% Ac_2O in NMP (*N*-methyl-2-pyrrolidinone) over 12 min at room temperature. Peptide cleavage and side-chain deprotection of amino acids were carried out by treating with TFA−ethanedithiol−thioanisole (18:1:1) over 2 h at room temperature.

Peptide Purification. Peptides synthesized above were purified by reversed-phase HPLC (column; COSMOSIL 5C18-AR-300 nacalai tesque, 10 × 150 mm) and elutes with 0.1% TFA buffer and a 10−50% CH_3CN (including 0.1% TFA) linear gradient (0−40 min) at a flow rate of 2.0 mL/min. The fraction of the peptides was monitored at 220 nm by a UV detector and identified with ESI-MS. MS (ESI) *m*/*z* peptide **A**: calcd for $C_{58}H_{96}N_{19}O_{21}$ ([M + H]$^+$) 1394.7, found 1394.9; peptide **B**: calcd for $C_{47}H_{79}N_{16}O_{16}$ ([M + H]$^+$) 1123.6, found 1123.5; peptide **C**: calcd for $C_{36}H_{62}N_{13}O_{11}$ ([M + H]$^+$) 852.5, found 852.1; peptide **D**: $C_{58}H_{96}N_{19}O_{21}$ ([M + H]$^+$) 1394.7, found 1395.0; peptide **E**: calcd for $C_{55}H_{94}N_{17}O_{21}$ ([M + H]$^+$) 1328.7, found 1327.9.

Cross-Linking Reaction. To a native peptide solution (0.5 mL; 1.0×10^{-3} M in 100 mM phosphate buffer, pH 6.6) was added **1** (0.5 mL; 2.0×10^{-3} M in DMSO). The reaction mixture was incubated at 50 °C in a thermomixer for 24 h. All of the cross-linked peptides were purified under similar conditions for peptide purification and identified by ESI-MS. MS (ESI) *m*/*z* **A·1**: calcd for $C_{70}H_{102}FeN_{19}O_{23}$ ([M + H]$^+$) 1632.7, found 1633.2; **B·1**: calcd for $C_{59}H_{85}FeN_{16}O_{18}$ ([M + H]$^+$) 1361.6, found 1361.7; **C·1**: calcd for $C_{48}H_{68}FeN_{13}O_{13}$ ([M + H]$^+$) 1090.4, found 1090.5; **D·1**: calcd for $C_{70}H_{102}FeN_{19}O_{23}$ ([M + H]$^+$) 1632.7, found 1633.2; **E·1**: calcd for $C_{67}H_{99}FeN_{19}NaO_{23}$ ([M + Na]$^+$) 1588.6, found 1587.6.

Electrochemical Analysis. All electrochemical measurements were carried out on a computer-controlled electroanalytical system at 25 °C by use of a conventional three-electrode cell, consisting of a saturated Ag/AgCl reference electrode, a platinum wire, and an Au electrode as a reference, an auxiliary, and a working electrode, respectively. The scanning speed was 100 mV/s. The solvent used in this analysis was 100 mM phosphate buffer including 100 mM $NaBF_4$ as an electrolyte.

Supporting Information Available: Beer's plot for **A·1**, cyclic voltammograms for **A·1**, **2**, and **Fc-(CO-Gly-OH)$_2$**, CD spectra of peptide **D** and **D·1**, UV/vis spectra of **2** in the presence of imidazole, and ^{1}H and ^{13}C NMR spectra of **1**. This material is available free of charge via the Internet at http://pubs.acs.org.

JO800117Q